

## Supporting Information

### **Amidoxime-Functionalized Microcrystalline Cellulose-Mesoporous Silica Composites for Carbon Dioxide Sorption at Elevated Temperatures**

Chamila Gunathilake,<sup>1</sup> Rohan S. Dassanayake,<sup>2</sup> Nouredine Abidi,<sup>\*2</sup> Mietek Jaroniec,<sup>\*1</sup>

<sup>1</sup> Department of Chemistry and Biochemistry, Kent State University, Kent, OH. 44242, USA.

E-mail: jaroniec@kent.edu

<sup>2</sup> Fiber and Biopolymer Research Institute, Department of Plant and Soil Science, Texas Tech University, Lubbock, TX, 79403, USA.

#### **Materials**

Microcrystalline cellulose (MCC) was donated by Fiber and Biopolymer Research Institute Lubbock, Texas. (3-cyanopropyl)triethoxysilane (CPS) was purchased from Alfa Aesar, Johnson Matthey Company, Ward Hill, Massachusetts. Hydroxylamine hydrochloride (NH<sub>2</sub>OH.HCl) was purchased from Sigma Aldrich. Pluronic P123 (EO<sub>20</sub>PO<sub>70</sub>EO<sub>20</sub>) triblock copolymer was donated by BASF Corporation, Florham Park, New Jersey. 95 % Ethanol, 36 % HCl, and NaOH were purchased from Fisher Scientific, Pittsburgh, Pennsylvania. Tetraethylorthosilicate (TEOS) was purchased from Gelest Inc., Morrisville, Pennsylvania. Deionized water (DW) was obtained using in house Ion pure Plus 150 Service Deionization ion-exchange purification system. All reagents were analytical grade and used without further purification.<sup>1-2</sup>

#### **Characterization**

Nitrogen adsorption isotherms were measured at -196 °C on an ASAP 2010 volumetric analyzer (Micromeritics, Inc., Norcross, GA). Prior to adsorption measurements, all samples were out gassed under vacuum at 110 °C for 2 h.<sup>1-4</sup>

High resolution thermogravimetric measurements were recorded on TGA Q-500 analyzer (TA Instruments, Inc., New Castle, DE). Thermogravimetric (TG) profiles were recorded from 25 to 720 °C in flowing nitrogen with a heating rate of 10 °C / min using a high resolution mode. The weight of each analyzed sample was typically in 5-15 mg range. The TG profiles were used to obtain information about the extent of the template removal, cyanopropyl functionalization, and amidoximation.<sup>1-4</sup>

Quantitative estimation of organic groups and N (%) was obtained by CHNS analysis using a LECO model CHNS-932 elemental analyzer (St. Joseph, MI).<sup>1,2,41</sup> H-<sup>13</sup>C cross polarization (CP) MAS NMR spectra were recorded using Bruker Avance (III) 400WB NMR spectrometer (Bruker Biospin Corporation, Billerica, MA, USA) with MAS triple resonance probe head using zirconia rotors 4 mm

in diameter.<sup>1,2,41</sup>  $^1\text{H}$ - $^{13}\text{C}$  CP-MAS NMR spectra were acquired at 400.13 MHz for  $^1\text{H}$  and 100.63 MHz for  $^{13}\text{C}$ . The MAS rate was 5 KHz.  $^1\text{H}$   $\pi/2$  pulse length was 3.5  $\mu\text{s}$  and pulse delay 2.0 s. TPPM20  $^1\text{H}$  decoupling sequence was used during acquisition. The  $^{13}\text{C}$  chemical shifts were referenced to p-dioxane 66.6 ppm.  $^1\text{H}$ - $^{29}\text{Si}$  cross polarization (CP) MAS NMR spectra were recorded at 79.49 MHz for  $^{29}\text{Si}$  and 400.13 MHz ( $^1\text{H}$ ). The MAS rate was 5 KHz.  $^1\text{H}$   $\pi/2$  pulse length was 4.5  $\mu\text{s}$  and pulse delay 3.0 s. Two pulse phase modulated TPPM15 decoupling sequence was used during acquisition. The  $^{29}\text{Si}$  chemical shifts were referenced to TMS (0 ppm).<sup>1-4</sup>

Transmission electron microscopy (TEM) images were obtained on a FEI Tecnai G2 F20 microscope. Prior to TEM analysis, the sample powders were dispersed in ethanol by moderate sonication at concentrations of ~5-10 wt. %. A Lacy carbon coated, 200-mesh, copper TEM grid was dipped into the sample suspension and then dried under vacuum at 80 °C for 20 h.<sup>1-3</sup> Field emission scanning electron microscopy (FE-SEM) images of the selected samples were observed using Hitachi S-4700 FE-SEM. Resolution of 1.5 nm at 15 kV can be achieved at 12 mm working distance and 2.5 nm at low kV (2 kV), at a working distance of 3 mm.

### **Room temperature CO<sub>2</sub> adsorption measurements**

CO<sub>2</sub> adsorption on the selected cyanopropyl- and amidoxime-containing MCC materials was measured in the pressure range up to 1.2 atm on ASAP 2020 volumetric adsorption analyzer (Micromeritics, Inc., GA) at 25 °C using ultrahigh purity (99.99 %) gaseous CO<sub>2</sub>. Prior to adsorption analysis each sample was outgassed at 110 °C for 2 h under vacuum.<sup>1-3</sup>

### **CO<sub>2</sub> chemisorption and TPD measurements**

CO<sub>2</sub> chemisorption and TPD experiments were conducted using a Micromeritics Auto Chem II Chemisorption Analyzer (Micromeritics, Inc., GA) equipped with a thermocouple detector (TCD). Approximately 20-100 mg of each sample were loaded in a quartz tube microreactor supported by quartz wool and subjected to pretreatment at 320 °C for 10 min before CO<sub>2</sub> adsorption, using a heating rate of 10 °C/min in flowing helium (at a rate of 50 cm<sup>3</sup>/min). Next, the sample was cooled to selected temperature (120 °C) using heating rate of 10 °C/min, exposed to pulse of 5 % CO<sub>2</sub>-He (50 cm<sup>3</sup>/min) as a loop gas, kept for 3 min and allowed for return to baseline. Recording was repeated until peaks are equal or 30 times. Recording was taken every 0.1 seconds and finally post CO<sub>2</sub> pulse purge was applied in flowing helium (50 cm<sup>3</sup>/min) for 30 min. In the TPD experiments, the samples were heated up to 320 °C using a heating rate of 5 °C/min and kept at this temperature for 90 min. The amounts of desorbed CO<sub>2</sub> were obtained by integration of the desorption profiles and referenced to the TCD signals calibrated for known volumes of analyzed gases.<sup>1-3</sup>

### **Calculations**

The Brunauer-Emmett-Teller specific surface areas ( $S_{\text{BET}}$ ) were calculated from the N<sub>2</sub> adsorption isotherms in the relative pressure range of 0.05-0.2 using a cross sectional area of 0.162 nm<sup>2</sup> per nitrogen molecule. The single-point pore volume ( $V_{\text{sp}}$ ) was estimated from the amount adsorbed at a relative pressure ( $p/p^0$ ) of ~ 0.98.<sup>1-4</sup> The pore size distributions (PSD) were calculated using adsorption branches of nitrogen adsorption-desorption isotherms by the improved KJS method calibrated for cylindrical

pores.<sup>5</sup>  $V_{mic}$ —volume of fine pores (micropores and small mesopores below 3 nm) calculated by integration of the PSD curve up to 3 nm. The pore width ( $W_{max}$ ) was obtained at the maximum of the PSD curve.<sup>1-4</sup>

**Table S1.** Comparison of the CO<sub>2</sub> uptake values reported for amine-functionalized and metal-incorporated sorbents at elevated temperatures.

Material	Sorption temperature (°C)	Maximum CO <sub>2</sub> uptake (mmol/g)	Reference
MgO/Al <sub>2</sub> O <sub>3</sub> composites	60	1.36	[6]
Zeolite based sorbents	120	1.20	[7]
Al-supported metal oxides (Ca, Mg, Ce, Cu, Cr)	120	1.80	[8]
Acetamidoxime/polyamidoxime	70	2.71	[9]
MgO-Al <sub>2</sub> O <sub>3</sub> aerogel	200	0.97	[10]
PEI/MCM 41	75	3.02	[11]
Hydrotalcite (mixed oxide of Ca, Al, Co, Mg)	350	1.39	[12]
K <sub>2</sub> CO <sub>3</sub> /MgO/Al <sub>2</sub> O <sub>3</sub>	60	2.49	[13]
Al incorporated organosilica	120	2.20	[4]
Amidoxime modified mesoporous silica	120	3.07	[1]
Amidoxime modified mesoporous silica	60	3.28	[1]
Microcrystalline cellulose based amidoxime	120	3.85	This work

## References

1. C. Gunathilake and M. Jaroniec, *Appl. Mater. Interfaces*, 2014, **6**, 13069–13078.
2. C. Gunathilake, J. Gorka, S. Dai and M. Jaroniec, *J. Mater. Chem. A*, 2015, **3**, 11650-11659.
3. C. Gunathilake and M. Jaroniec, *J. Mater. Chem. A*, 2015, **3**, 2707-2716.
4. C. Gunathilake, M. Gangoda and M. Jaroniec, *J. Mater. Chem. A*, 2013, **1**, 8244-8252.
5. M. Kruk, M. Jaroniec and A. Sayari, *Langmuir*, 1997, **13**, 6267-6273.
6. L. Li, X. Wen, X. Fu, F. Wang, N. Zhao, F. Xiao, W. Wei and Y. Sun, *Energy Fuels*, 2010, **24**, 5773.
7. R. V. Siriwardena, M. S. Shen and E. P. Fisher, *Energy Fuels*, 2005, **19**, 1153.
8. W. Cai, J. Yu, C. Anand, A. Vinu and M. Jaroniec, *Chem. Mater.*, 2011, **23**, 1147.
9. C. Zulfiqar, F. Karadas, J. Park, E. Deniz, G. D. Stucky and Y. Jung, *Energy Environ. Sci.*, 2011, **4**, 4528.
10. S. J. Han, Y. Bang, H. J. Kwon, H. C. Lee, V. Hiremath, I. K. Song and J. G. Seo., *Chem. Eng. J.*, 2014, **242**, 357.
11. X. Xu, C. Song, B. G. Miller and A. W. Scaroni, *Ind. Eng. Chem. Res.*, 2005, **44**, 8113.
12. X. P. Wang, J. J. Yu, J. Cheng, Z. P. Hao and Z. P. Xu, *Environ. Sci. Technol.*, 2008, **42**, 614.
13. L. Li, Y. Li, X. Wen, F. Wang, N. Zhao, F. Xiao, W. Wei and Y. Sun, *Energy Fuels*, 2011, **25**, 3835.

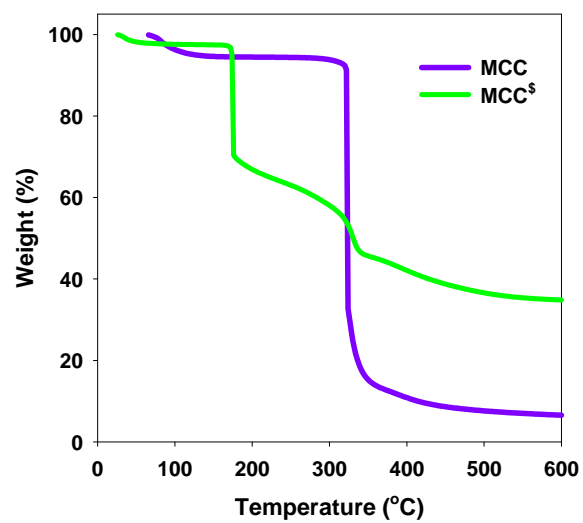


**Figure S1.** TG curves for the microcrystalline cellulose (MCC) and the MCC<sup>S</sup> sample prepared using MCC and TEOS.

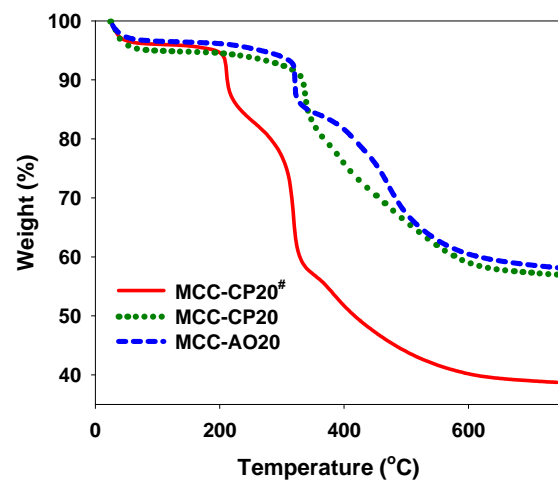


**Figure S2.** TG curves for the as-synthesized (MCC-CP20<sup>#</sup>), cyanopropyl-functionalized (MCC-CP20), and amidoxime-modified MCC (MCC-AO20) samples.

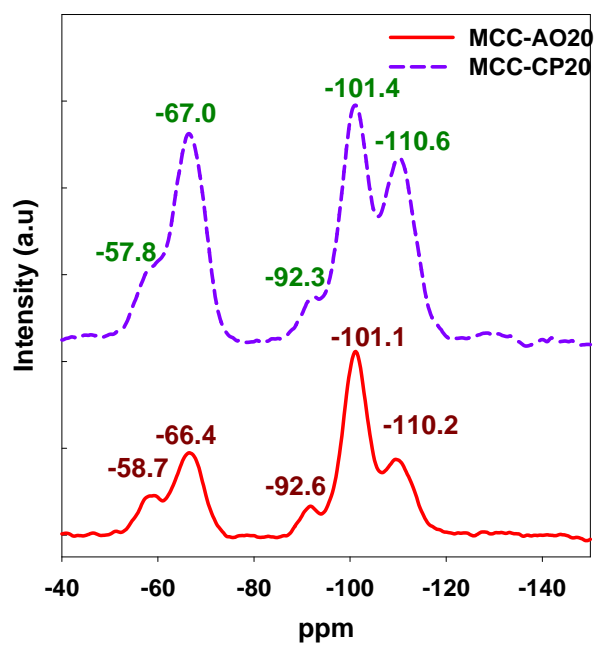


**Figure S3.**  $^{29}\text{Si}$  MAS NMR spectra of MCC-CP20 and MCC-AO-20.

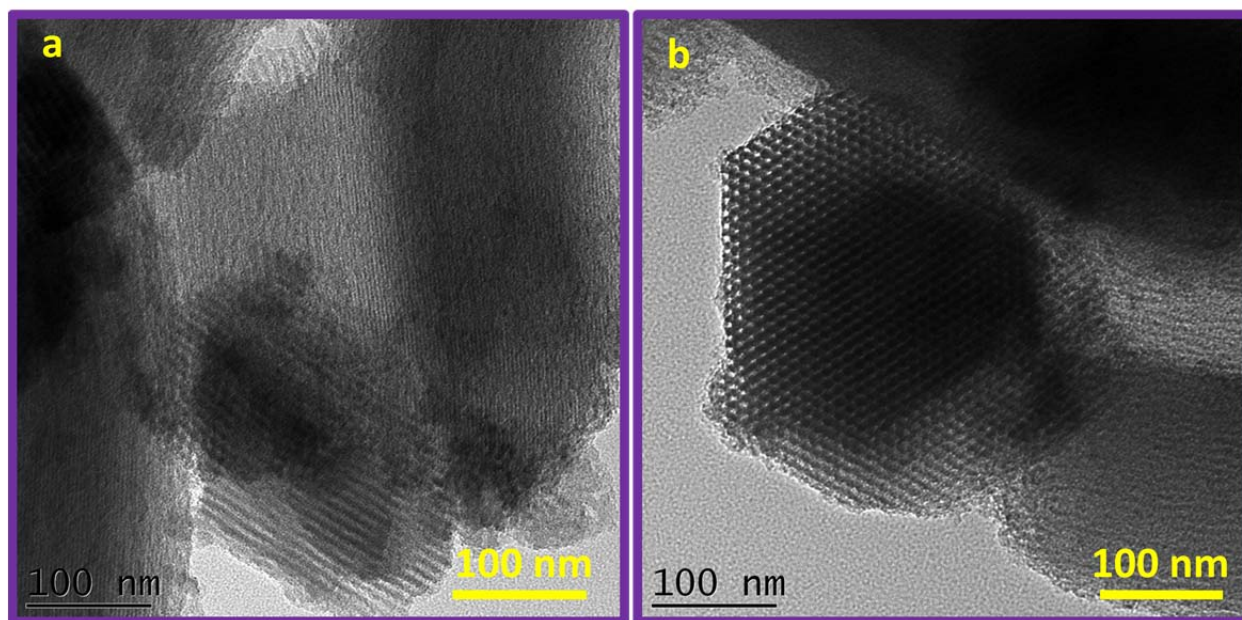


**Figure S4.** TEM images of the MCC-CP20 (a) and MCC-AO20 (b) samples.

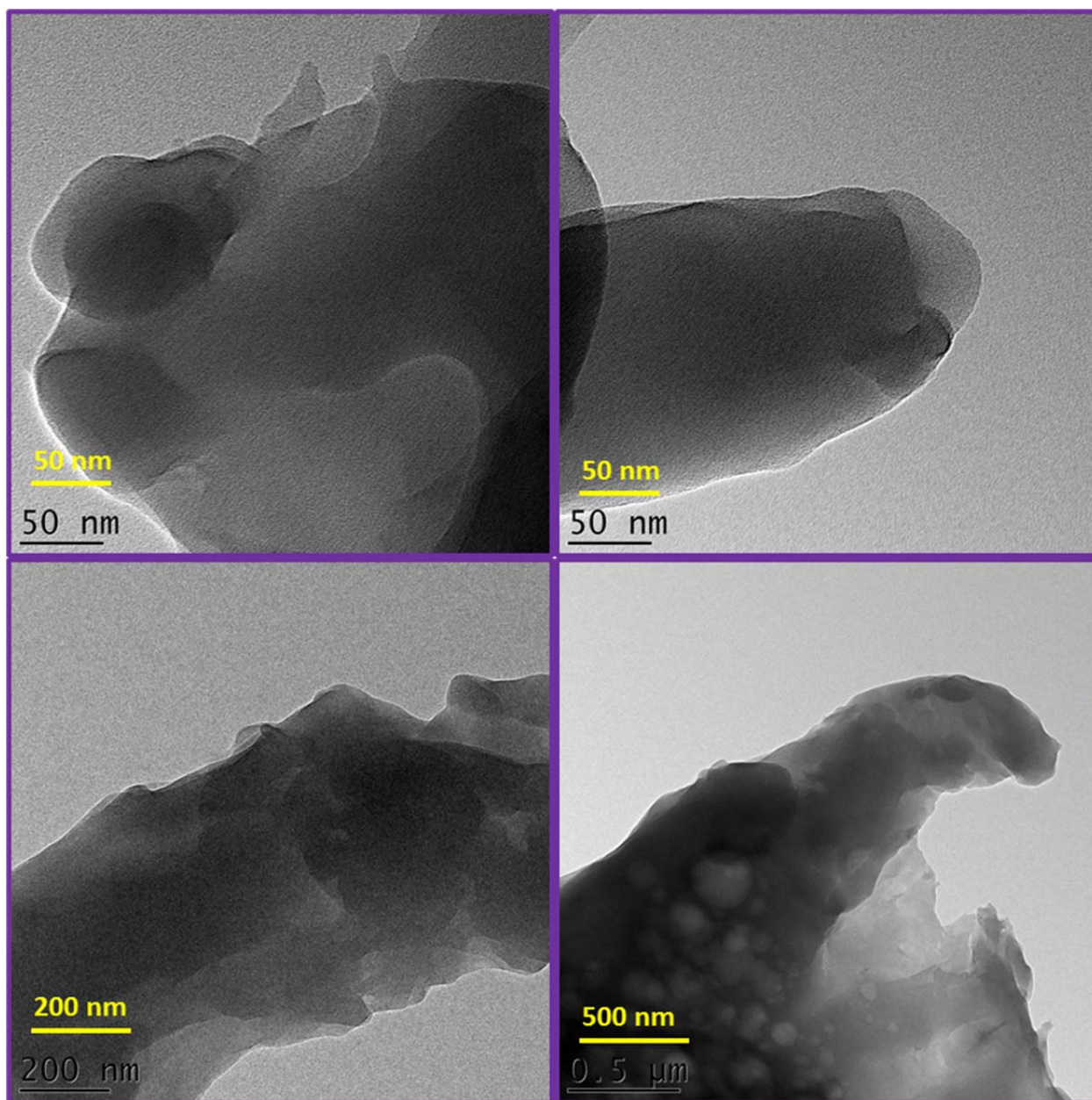


**Figure S5.** TEM images of the MCC sample.



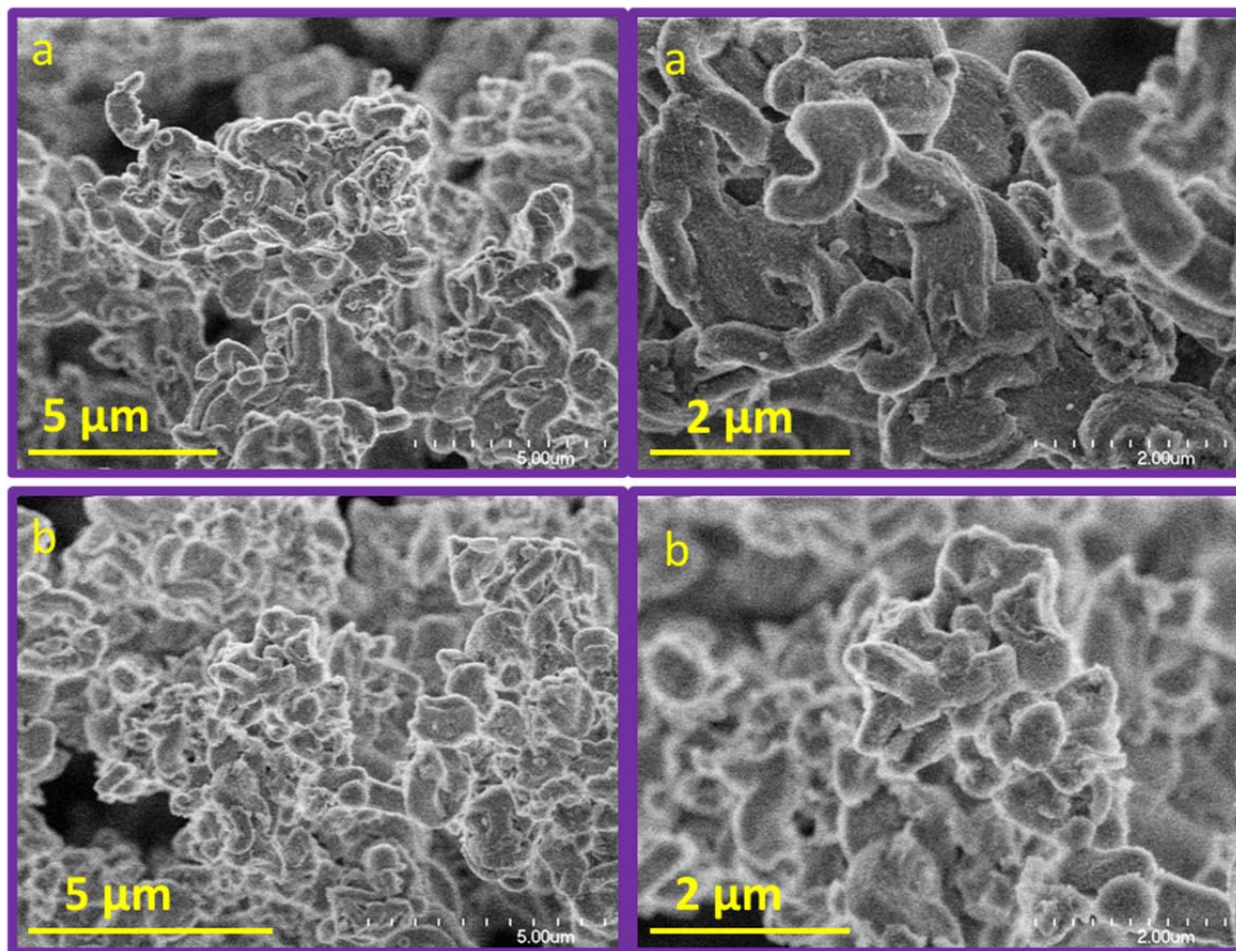


**Figure S6.** SEM images of the MCC-CP10 (a, top panels) and MCC-AO10 (b, bottom panels) samples.

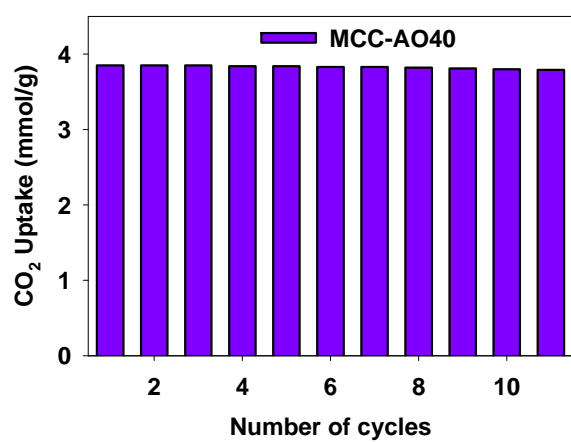
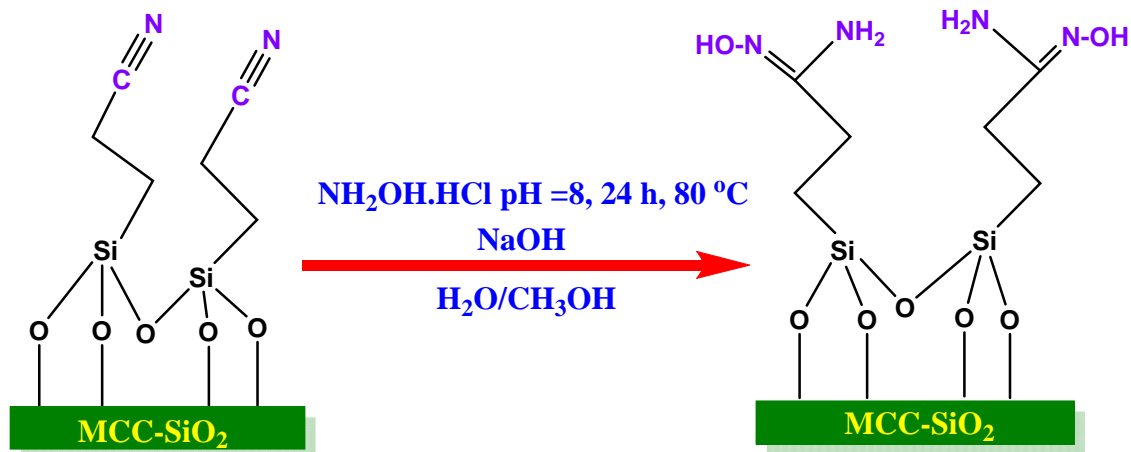
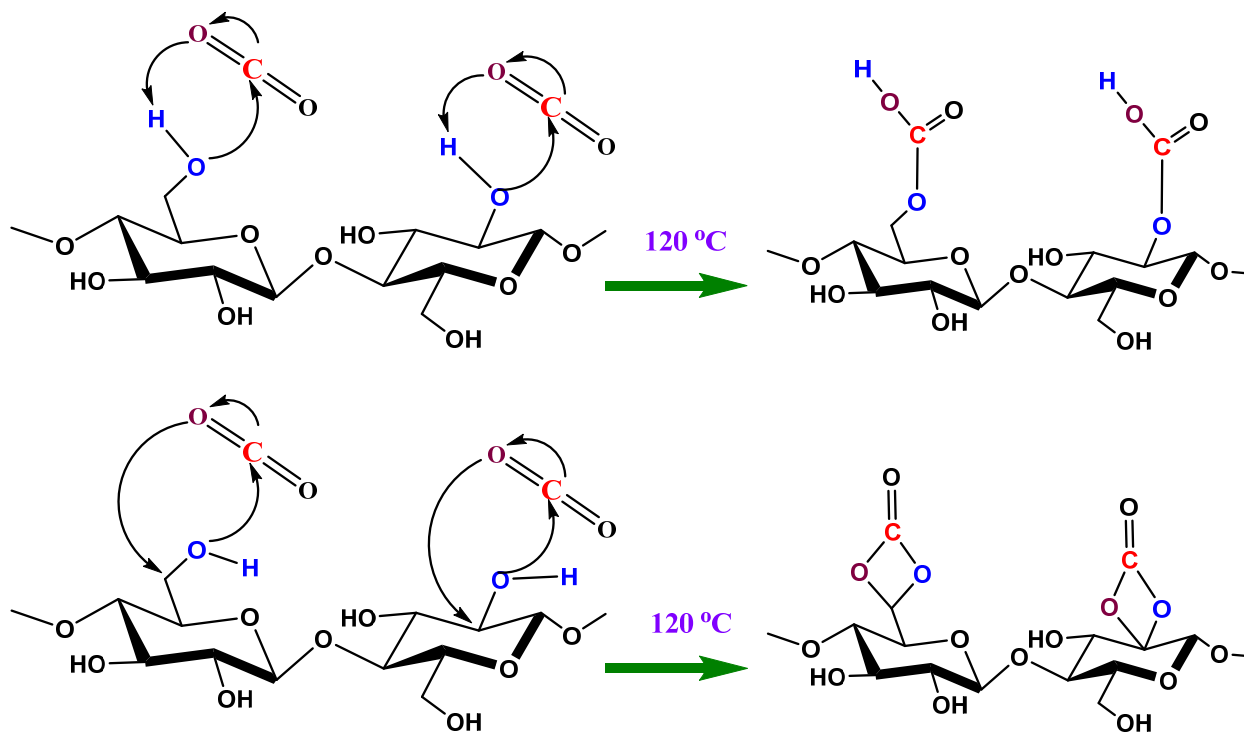


**Figure S7.** Cycle stability of MCC-AO40.

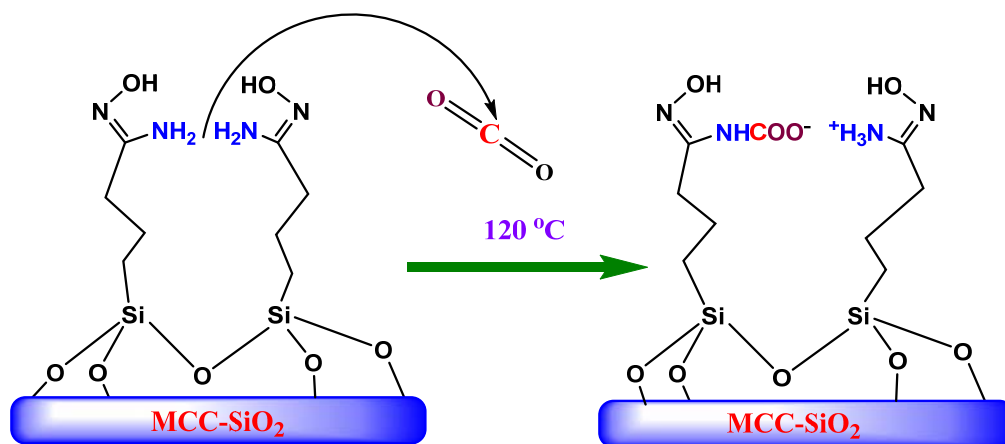


**Scheme 1.** Systematic illustration showing conversion of CP-MCC to AO-MCC in the presence of hydroxylamine hydrochloride.<sup>1,2</sup>



**Scheme 2.** Schematic illustration of possible hydrogen carbonate (top) and bidentate carbonate (bottom) formation upon  $\text{CO}_2$  chemisorption on MCC.





**Scheme 3.** Schematic illustration of CO<sub>2</sub> binding on the amidoxime-modified MCC at 120 °C.